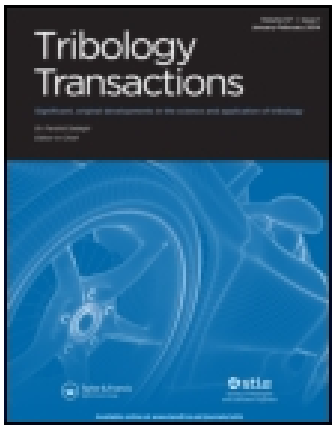

Tribology Transactions
Publication details, including instructions for authors and subscription information:
http://www.tandfonline.com/loi/utrb20

Synergetic Lubricating Effect of WS_2 and Ti_3SiC_2 on Tribological Properties of Ni_3Al Matrix Composites at Elevated Temperatures

Wenzheng Zhai[a], Xiaoliang Shi[a], Jie Yao[a], Zengshi Xu[a], Ahmed Mohamed Mahmoud Ibrahim[a], Qingshuai Zhu[a], Long Chen[a] & Yecheng Xiao[a]
[a] School of Mechanical and Electronic Engineering, Wuhan University of Technology, Wuhan 430070, China
Accepted author version posted online: 10 Dec 2014.Published online: 04 Feb 2015.

To cite this article: Wenzheng Zhai, Xiaoliang Shi, Jie Yao, Zengshi Xu, Ahmed Mohamed Mahmoud Ibrahim, Qingshuai Zhu, Long Chen & Yecheng Xiao (2015) Synergetic Lubricating Effect of WS_2 and Ti_3SiC_2 on Tribological Properties of Ni_3Al Matrix Composites at Elevated Temperatures, Tribology Transactions, 58:3, 454-466, DOI: 10.1080/10402004.2014.986353

To link to this article: http://dx.doi.org/10.1080/10402004.2014.986353

Tribology Transactions, 58: 454–466, 2015

ISSN: 1040-2004 print / 1547-397X online
DOI: 10.1080/10402004.2014.986353

stle
Society of Tribologists and Lubrication Engineers

Synergetic Lubricating Effect of WS_2 and Ti_3SiC_2 on Tribological Properties of Ni_3Al Matrix Composites at Elevated Temperatures

WENZHENG ZHAI, XIAOLIANG SHI, JIE YAO, ZENGSHI XU, AHMED MOHAMED MAHMOUD IBRAHIM, QINGSHUAI ZHU, LONG CHEN, and YECHENG XIAO
School of Mechanical and Electronic Engineering, Wuhan University of Technology, Wuhan 430070, China

The tribological behaviors of the Ni_3Al-WS_2-Ti_3SiC_2 composites and synergistic effect of composite solid lubricants are investigated from room temperature to 800°C. The results show that the Ni_3Al matrix composites (NASC) exhibit excellent tribological properties throughout the test temperatures compared to Ni_3Al-based alloy. The excellent tribological properties of NASC are attributed to the synergistic lubricating effect of WS_2 and Ti_3SiC_2. A lubricating film could be formed below 400°C, and an oxidation protection film is formed above 400°C on the worn surface of NASC during the sliding process, leading to low coefficients of friction (0.18–0.39) and wear rates ($1.5–3.7 \times 10^{-5}$ $mm^3N^{-1}m^{-1}$).

KEY WORDS

Solid Lubrication Friction, Self-Lubricating Composites, Coupling Lubricants, Wear Mechanisms

INTRODUCTION

High friction often leads to high wear losses and, hence, shorter life and poor reliability in moving mechanical systems (Berman, et al. *(1)*). Consequently, friction and wear is one of the most active fields of study. In an effort to improve the tribological properties of the materials used in moving mechanical systems, many attempts have been made to develop new materials with satisfactory self-lubricating properties. Among them, metal matrix self-lubricating composites that possess superior antifriction and wear resistance have been one of the core issues of advanced material research (Evans and Senior *(2)*; Prasad and Mecklenburg *(3)*).

Ni_3Al is regarded as potential high-temperature structural material due to its high melting point and good high-temperature mechanical properties, as well as excellent corrosion and oxidation resistance (Sierra and Vazquez *(4)*). However, the tribological properties need to be enhanced for Ni_3Al as the candidate for structural components. The addition of effective solid lubricants becomes an ideal solution to improve the tribological properties of Ni_3Al matrix composites. Zhu, et al. *(5)* investigated the tribological properties of Ni_3Al matrix composites (NASC) with various $BaCrO_4$ contents. The results showed that NASC had a low wear rate at high temperatures due to the oxidative layer consisting of NiO and $BaCrO_4$ that re-formed on the worn surface. According to previous research results, Ni_3Al matrix composites containing only a solid lubricant do not possess excellent tribological properties over a wide temperature range, because the application of a solid lubricant is limited by the temperature and most lubricants are oxidized at high temperature. For instance, molybdenum disulfide is oxidized at temperatures higher than 500°C, graphite loses its lubricating role at temperatures above 450°C, and rare earth compounds are effective at room temperature (Li, et al. *(6)*). Solid lubrication over a wide temperature range has been a long challenge for tribologists. Many researchers are still working to design materials with satisfactory self-lubricating properties over a wide temperature range to meet the requirements for industrial applications, such as self-lubricant bearings, gears, pulleys, and other components (Sliney *(7)*; Ouyang, et al. *(8)*; Dellacorte *(9)*).

One of the most effective ways is to combine low-temperature lubricants with high-temperature lubricants in the matrix materials to achieve low coefficients of friction and wear rates over a wide temperature range. Li, et al. *(6)* investigated the effect of Ag and CeO_2 on the friction and wear properties of Ni-based composites at high temperature. They observed that the coefficient of friction from room temperature (RT) to 400°C was reduced by adding Ag in the Ni-based composite and the addition of CeO_2 was favorable to the formation of a smooth tribolayer during high-temperature friction, which reduced friction and wear at 600°C. Tyagi, et al. *(10)* studied the elevated temperature tribological behavior of Ni-based composites containing nano-silver and hBN. They found that the coefficients of friction of silver- and hBN-containing composites were observed to be lower than that of the base alloy with no lubricant at all temperatures, which was attributed to the presence of solid lubricants and their synergy.

To the best of the authors' knowledge, compared to the extensive studies of Ni-based self-lubricating composites over a wide temperature range, only a few studies have focused on NASC. Zhu, et al. *(11)* successfully fabricated an Ni_3Al matrix high-

Manuscript received August 5, 2014
Manuscript accepted November 3, 2014
Review led by David Burris
Color versions of one or more of the figures in the article can be found online at www.tandfonline.com/utrb.

temperature self-lubricating composite Ni_3Al-BaF_2-CaF_2-Ag-Cr using a powder metallurgy technique. The composite exhibited low coefficients of friction and wear rates from RT to 800°C, which were attributed to the synergistic effects of Ag, fluorides, and chromates formed on the worn surfaces by the tribochemical reaction. This indicated that Ni_3Al might be an excellent matrix for elevated temperature self-lubricating composites. Therefore, the tribological behavior of NASC with the appropriate solid lubricants over a wide temperature range requires more research.

The solid lubricant WS_2 has a lamellar structure like MoS_2 and graphite and is easily sheared, forming lubricious transfer films between the friction pair interface. In addition, WS_2 has a relatively high oxidation temperature (539°C) compared to MoS_2 (370°C) or graphite (325°C), so it can maintain lubrication at relatively higher temperatures (Yang, et al. *(12)*). As a new solid self-lubricating material, Ti_3SiC_2 combines many of the best properties of both ceramics and metals (Shi, et al. *(13)*). It has been proved to be a promising tribological material at high temperatures with a low coefficient of friction and wear rate (Zhang, et al. *(14)*; Shi, et al. *(15)*). The good tribological properties are attributed to the formation of a lubricious oxide film on the Ti_3SiC_2 tribosurface (Barsoum, et al. *(16)*). WS_2 can provide good lubricity at low temperature and Ti_3SiC_2 can provide good lubricity at high temperature. The synergetic lubricating effect of WS_2 and Ti_3SiC_2 (WT) may ensure that NASC possesses a low coefficient of friction and wear rate over a wide temperature range.

In this article, NASC containing varying amounts of WT with a weight ratio of 1:1 were fabricated by an in situ technique using spark plasma sintering (SPS). The objective of this article is to design and fabricate high-temperature self-lubricating composites with excellent tribological properties, as well as to explore the self-lubricating and wear mechanisms over a wide temperature range from RT to 800°C. The effects of different contents of WT on the friction and wear behavior of NASC have been experimentally studied during friction and wear tests at a load of 10 N and sliding speed of 0.2 m/s for 80 min from RT to 800°C on a pin-on-disk high-temperature tribometer. For comparison, the tribological properties of NASC with each lubricant at 5 and 10 wt% are also tested under the same conditions.

EXPERIMENTAL DETAILS

Material Preparation

The composite Ni_3Al powders were composed of commercially available Ni, Al, Cr, Mo, Zr, and B powders with an average particle size of about 30–50 μm an atomic ratio of 4.5Ni : 1Al : 0.333Cr : 0.243Mo : 0.0047Zr : 0.0015B. WS_2 powders were purchased from Nanjing XFNANO Materials Tech Co., Ltd. The average grain size of WS_2 powders was about 20–40 μm. Ti_3SiC_2 powders were produced by vacuum solid state reaction in our laboratory (Peng, et al. *(17)*). The average grain size of Ti_3SiC_2 powders was about 5–10 μm. The weight fractions of WS_2 and Ti_3SiC_2 in NASC were fixed at 0, 2.5, 5, and 7.5 wt%, respectively. Hence, the total percentages of solid lubricants in NASC were fixed to be 0, 5, 10, and 15 wt%, respectively. The compositions of the as-prepared samples are listed in Table 1. NASC without lubricants is denoted by NA. NASC with 5, 10, and 15 wt% WT are denoted by NA-5WT, NA-10WT, and NA-15WT, respectively. NASC with 5 and 10 wt% WS_2 are denoted by NA-5W and NA-10W. Moreover, NASC with 5 and 10 wt% Ti_3SiC_2 are denoted by NA-5T and NA-10T. The starting powders were mixed together by high-energy ball-milling in a vacuum for 10 h. Balls and vials were made of hard alloy, and the charge ratio (ball-to-powder mass ratio) employed was 10:1. After being mixed and dried, the mixed powders were enclosed in a cylindrical graphite mold with an inner diameter of 20 mm and then sintered by SPS using a D.R. Sinter SPS3.20 (Sumitomo Coal & Mining, now SPS Syntex Inc.) apparatus at 1100°C under a pressure of 35 MPa for 12 min in pure Ar atmosphere protection. The as-prepared specimen surfaces were ground to remove the layers on the surfaces and polished mechanically with successive grades of emery paper down to 1,200 grit, followed by wet polishing with 5-μm diamond pastes to a mirror finish. The measured density of each as-produced sample was determined by Archimedes' principle according to ASTM Standard B962–13 (American Society for Testing and Materials *(18)*). Eight tests were conducted and the mean value and standard deviation are provided. The Vicker's microhardness of each as-produced sample was measured using an HVS-1000 Vicker's hardness instrument with a load of 1 kg and a dwell time of 8 s according to ASTM Standard E384–11e1 (American Society for Testing and Materials *(19)*). Eight tests were conducted and the mean value and standard deviation are provided.

Tribological Test

Dry friction and wear tests were carried out on an HT-1000 high-temperature pin-on-disk tribometer (Zhong Ke Kai Hua Corporation, China) according to ASTM Standard G99–05 (American Society for Testing and Materials *(20)*). The disk, which was the as-prepared sample, rotated with a constant speed. The counterface ball was a commercially available ball of Si_3N_4 (15.0 GPa), which was polished to an average surface roughness (R_a) of 0.01 μm. The Si_3N_4 ball was used as the counterpart

TABLE 1—COMPOSITIONS, MICROHARDNESS, AND DENSITY OF THE AS-PREPARED SAMPLES

Sample	Composition (wt%)	Microhardness (GPa)	Density (g/mm^3)	Relative Density (%)
NA	Ni_3Al	5.17	7.38	98.7
NA-5WT	Ni_3Al-2.5WS_2-2.5Ti_3SiC_2	5.72	7.35	98.3
NA-10WT	Ni_3Al-5WS_2-5Ti_3SiC_2	6.45	7.24	97.6
NA-15WT	Ni_3Al-7.5WS_2-7.5Ti_3SiC_2	6.11	7.12	96.3

during the sliding tests because (1) the hard Si_3N_4 ball could ensure that plastic deformation occurred within the composites, hence reflecting the wear resistance mechanism of NASC; and (2) the Si_3N_4 ceramic had good resistance to high-temperature oxidation and good mechanical behavior under elevated temperatures. The disks and counterface balls were cleaned with an acetone solution and then dried in hot air before the sliding wear tests. Sliding tests at the selected temperatures of RT, 200°C, 400°C, 600°C, and 800°C were carried out at an applied load of 10 N, sliding speed of 0.2 m/s, and testing time of 80 min. The coefficients of friction were automatically measured and recorded in real time by the friction tester' computer system. The cross-section profile of worn surface was measured using a surface profilometer. The wear volume V was determined as $V = AL$, where A is the cross-sectional area of wear scar, and L is the perimeter of wear scar. The wear rate was calculated by the formula $W = V/SF$, where V is the wear volume, S is the sliding distance, and F is the normal load. This was calculated as a function of the wear volume divided by the sliding distance S and the applied load F (expressed as $mm^3N^{-1}m^{-1}$). The tests for each given condition were repeated three times to assess the variability of the data.

Microstructure Analysis

The surface of the as-prepared samples was examined by X-ray diffraction (XRD) with Cu Kα radiation at 30 kV and 40 mA at a scanning speed of 0.01 s^{-1} for identification of the phase constitution. The morphologies and compositions of the worn surfaces of the samples obtained at different temperatures were analyzed using electron probe microanalysis (EPMA; JAX-8230) and energy-dispersive spectroscopy (EDS; Genesis 7000). The phases of the worn surfaces of NA-5WT at 200°C and NA-10WT at 600°C were analyzed by a VG Multilab 2000 X-ray photoelectron spectroscope (XPS). The morphologies and compositions of cross sections of the wear scars of NA-10WT obtained at 400°C were analyzed by a field emission scanning electron microscope (FESEM; FEI-SIRION) and EDS. The microstructure and elemental distribution of cross sections of the wear scars of NA-10WT obtained at 400°C were also observed and analyzed by EPMA.

RESULTS AND DISCUSSION

Microstructural and Mechanical Properties

XRD patterns of the as-prepared NA, NA-5WT, NA-10WT, and NA-15WT are presented in Fig. 1. It can be seen that the diffraction peaks primarily belong to the Ni_3Al phase in all samples. Moreover, the C phase can be found, which indicates that carburization has occurred during the SPS process. In addition to the Ni_3Al and C phases, lubricating phases of WS_2 and Ti_3SiC_2 can be found in NA-5WT, NA-10WT, and NA-15WT. Due to the decomposition reaction or impurity of Ti_3SiC_2, the new phase of TiC appears in NA-5WT, NA-10WT, and NA-15WT. The enhanced phase of TiC can effectively reduce the wear rate and enhance the wear resistance of the composites because of its high hardness (Yang, et al. *(21)*).

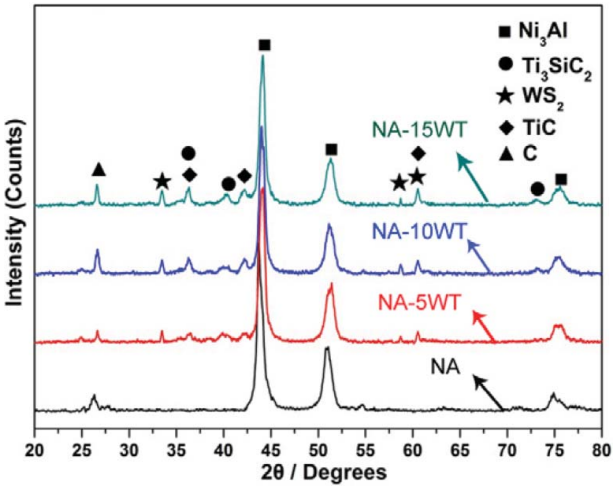

Fig. 1—XRD patterns of the as-prepared NA, NA-5WT, NA-10WT, and NA-15WT.

The typical microstructures and elemental distributions of NA and NA-10WT are shown in Figs. 2 and 3, respectively. Analysis of the elemental distribution shows that the Ni_3Al phase has a dense and uniform distribution in the samples, and the WS_2 and Ti_3SiC_2 phases have a scattered distribution. According to the elemental distribution and EDS analysis, the gray area is the continuous bulk Ni_3Al phase, the white area is the WS_2 phase, and the dark gray area is the Ti_3SiC_2 phase. The isolated WS_2 and Ti_3SiC_2 phases are surrounded by the continuous bulk Ni_3Al phase in NA-10WT, which could contributed to the excellent lubrication role of NA-10WT.

Table 1 lists the composition, microhardness, and density of the as-prepared samples. It can be seen that the densities of the as-prepared samples decrease with an increase in the lubricant content. This is mainly due to the fact that the density of Ti_3SiC_2 is less than that of NiAl. Moreover, the addition of WS_2 and Ti_3SiC_2 improves the hardness of NASC. This may be attributed to the presence of a TiC reinforcement phase. The results show that NA-10WT has the highest hardness of 6.45 GPa.

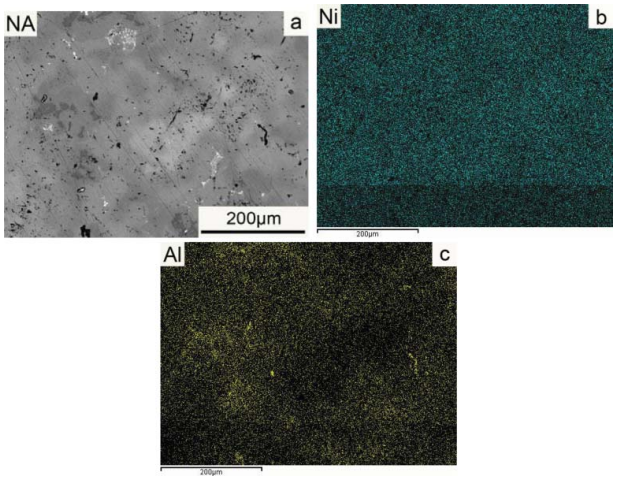

Fig. 2—Typical microstructure and elemental distribution of NA.

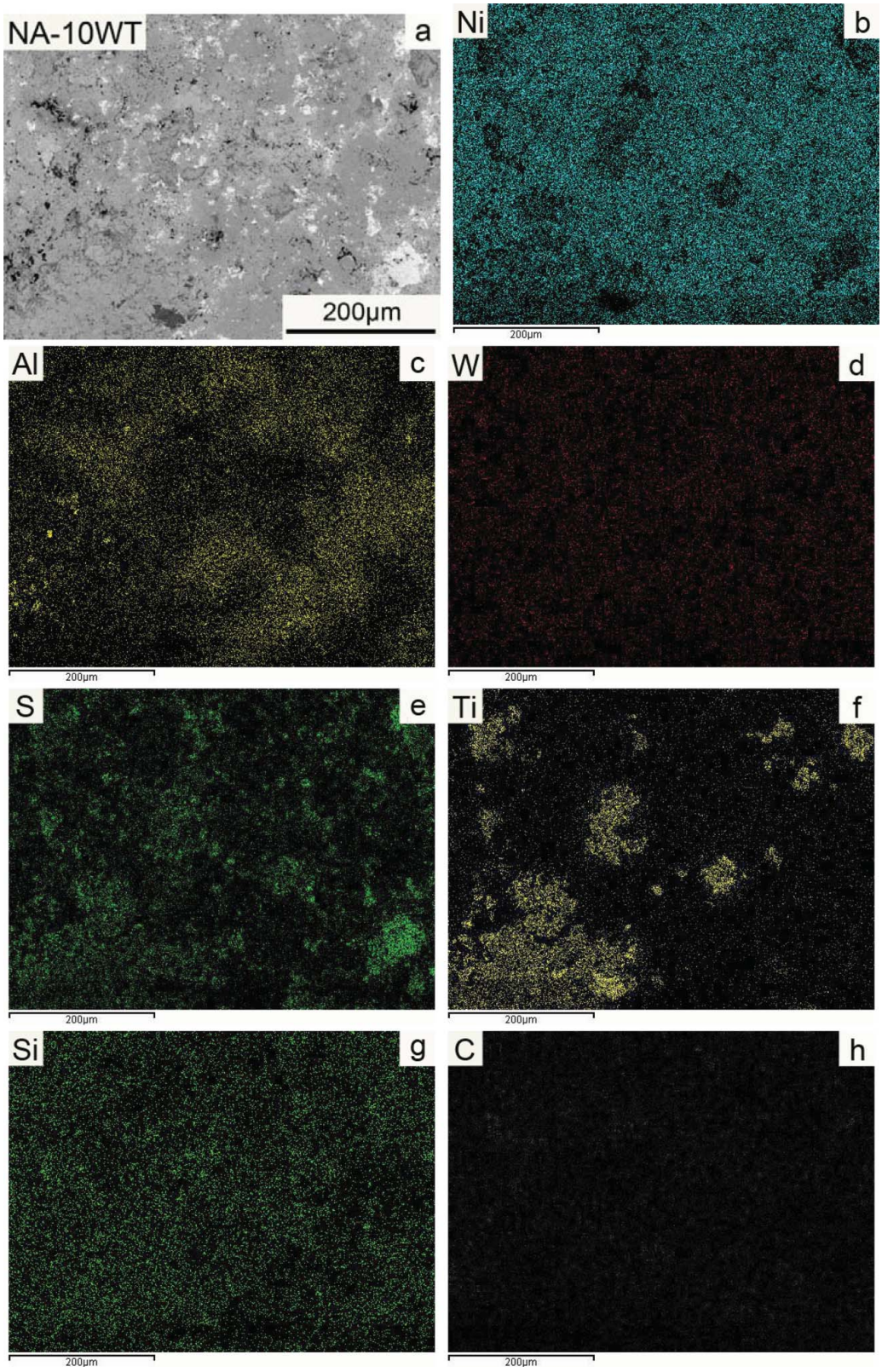

Fig. 3—Typical microstructure and elemental distribution of NA-10WT.

Friction and Wear Behavior

Figure 4a shows the variations in the coefficients of friction of the as-prepared NA, NA-5WT, NA-10WT, and NA-15WT with a sliding time of 80 min at different temperatures under an applied load of 10 N and a sliding velocity of 0.2 m/s. For the purpose of comparison, Fig. 4b shows the coefficients of friction of NA-5W, NA-10W, NA-5T, and NA-10T under the same conditions. The error bars are the standard deviations of the average

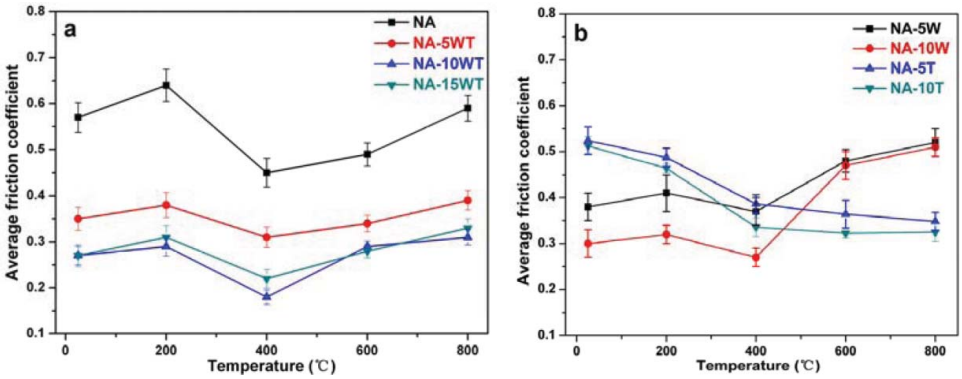

Fig. 4—Variations in the coefficients of friction of the (a) as-prepared NA, NA-5WT, NA-10WT, and NA-15WT and (b) NA-5W, NA-10W, NA-5T, and NA-10T from RT to 800°C.

coefficients of friction. The coefficients of friction of NASC gradually decrease to a low value at temperatures from RT to 400°C and then increase from 400 to 800°C. It can be seen that the coefficients of friction of NA are the highest in all of the as-prepared samples for all test temperatures. As can be seen from Fig. 4a, the coefficient of friction of NA is observed to increase from 0.57 to 0.64 when the temperature increases from RT to 200°C, and as the temperature increases to 400°C, it reaches its a minimum value of 0.45. It then increases gradually from 0.49 to 0.59 as the temperature increases from 600 to 800°C. The coefficients of friction of NA-5WT, NA-10WT, and NA-15WT obviously decrease less compared to NA for all test temperatures with the addition of the solid lubricants WS_2 and Ti_3SiC_2, especially for NA-10WT. The coefficients of friction of NA-5WT are in the range of 0.31–0.39 from RT to 800°C. For NA-10WT, it is distinctly seen that the coefficients of friction are lower than those of the above two (NA and NA-5WT) and in the range of 0.18–0.31 from RT to 800°C. Additionally, the coefficients of friction of NA-15WT are in the range of 0.22–0.33 from RT to 800°C. However, with an increase in WS_2 and Ti_3SiC_2 from 10 to 15 wt%, the coefficients of friction did not obviously decrease. As shown in Fig. 4a, the coefficient of friction of NA-15WT is higher than that of NA-10WT at 200, 400, and 800°C. The coefficient of friction is observed to increase from 0.29 to 0.31 at 200°C, from 0.18 to 0.22 at 400°C, and from 0.31 to 0.33 at 800°C. For NASC with each lubricant at 5 and 10 wt%, as shown in Fig. 4b, the coefficients of friction vary from about 0.30 to 0.54 from RT to 800°C. NA-5W and NA-10W show high coefficients of friction at 600°C (about 0.49) and 800°C (about 0.54) compared to NA-10WT. NA-5T and NA-10T have relatively high values at RT (about 0.53) and 200°C (about 0.51).

Figure 5a shows the variations in wear rates of the as-prepared NA, NA-5WT, NA-10WT, and NA-15WT at different temperatures after the tests. Figure 5b shows the wear rates of NA-5W, NA-10W, NA-5T, and NA-10T under the same conditions. The error bars are the standard deviations of the average wear rates. It can be seen that the wear rates of NA are apparently the highest in all of the as-prepared samples for all test temperatures. As can be seen from Fig. 5a, the wear rates of NA are in the range of 4.3–6.1 $\dot{c}$ 10^{-5} $mm^3N^{-1}m^{-1}$ from RT to 800°C. Compared to NA, the other three samples have lower wear rates for all test temperatures. It can be seen that the wear rates of NA-5WT, NA-10WT, and NA-15WT show a similar variation trend with an increase in temperature. The wear rate of NA-5WT is about 3.2 $\dot{c}$ 10^{-5} $mm^3N^{-1}m^{-1}$ at RT; it increases to the highest value of 3.7 $\dot{c}$ 10^{-5} $mm^3N^{-1}m^{-1}$ at 200°C and then sharply decreases to the lowest value of 2.7 $\dot{c}$ 10^{-5} $mm^3N^{-1}m^{-1}$ at 400°C. As the temperature increases from 600 to 800°C, it increases gradually from 3.2 to 3.4 $\dot{c}$ 10^{-5} $mm^3N^{-1}m^{-1}$. For NA-10WT, the wear rates are the lowest in all of the as-prepared

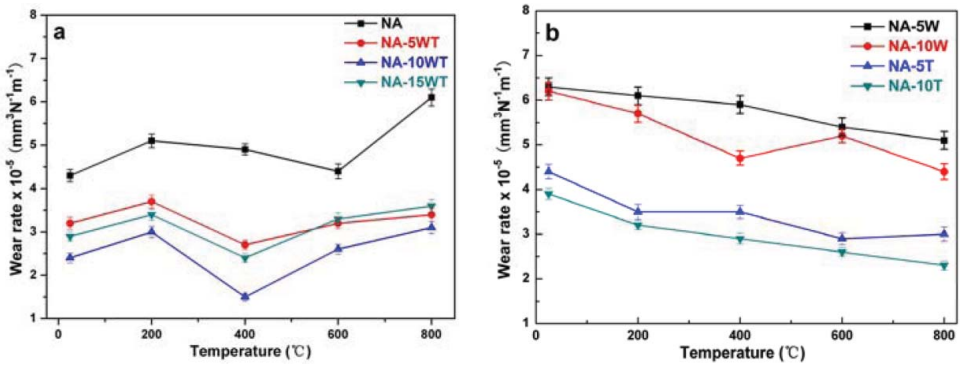

Fig. 5—Variations in the wear rates of the (a) as-prepared NA, NA-5WT, NA-10WT, and NA-15WT and (b) NA-5W, NA-10W, NA-5T, and NA-10T from RT to 800°C.

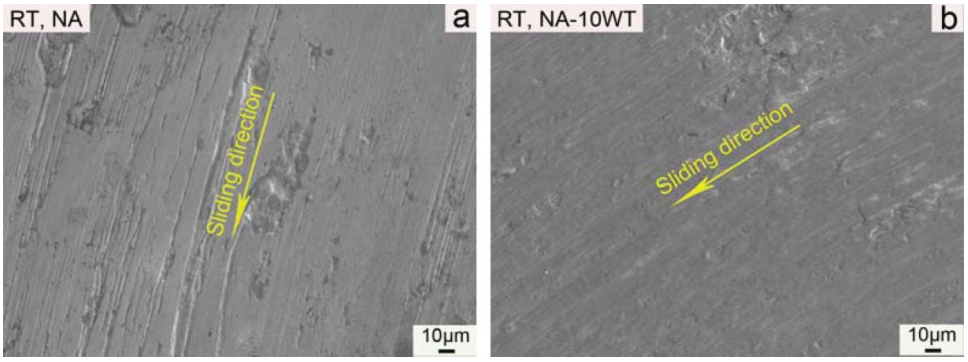

Fig. 6—Wear track morphologies of NA and NA-10WT after sliding tests at RT.

samples and in the range of 1.5–3.1 ċ 10^{-5} $mm^3N^{-1}m^{-1}$ from RT to 800°C. Additionally, the wear rates of NA-15WT are in the range of 2.4–3.6 ċ 10^{-5} $mm^3N^{-1}m^{-1}$ from RT to 800°C. As shown in Fig. 5b, NA-5W and NA-10W show relatively low wear resistance compared to NA-10WT. The wear rates of NA-5W and NA-10W are about 4.9–6.3 ċ 10^{-5} $mm^3N^{-1}m^{-1}$. NA-5T and NA-10T exhibit good wear resistance at relatively high temperatures. The wear rates of NA-5T and NA-10T at low temperatures are higher than those of NA-10WT.

The aforementioned friction and wear results have shown that both the coefficients of friction and wear rates of NA-5WT, NA-10WT, and NA-15WT are reduced for all test temperatures. This indicates that WS_2 and Ti_3SiC_2 solid lubricants added to the NiAl matrix are capable of producing a noticeable reduction in friction and wear from RT to 800°C. In addition, there is an optimum content of solid lubricants in self-lubricating composites under a given set of conditions that contributes to excellent tribological properties, which generally means a low coefficient of friction and wear rate. According to the above analysis, NA-10WT has the best tribological properties under the conditions used in the study. The self-lubricating and wear mechanisms of NA-10WT are discussed in further detail in the following subsections.

Worn Surfaces and Cross Section

Figure 6 shows the wear track morphologies of NA and NA-10WT after sliding tests at RT. As shown in Fig. 6a, the deep scratches and potholes on the smooth worn surface of NA suggest that the main wear mechanism is adhesion at RT. As shown in Fig. 6b, the worn surface of NA-10WT is covered by a smooth and dense tribofilm formed during the sliding process because abundant wear debris particles adhere on the worn surface. Moreover, the EDS analysis reveals that the tribofilm contains an abundance of W (5.07 wt%) and S (1.74 wt%) elements, indicating the presence of WS_2 which may have acted as a lubricant during the sliding process. This may explain the lower coefficient of friction of NA-10WT compared to NA.

Figure 7 shows the wear track morphologies of NA and NA-10WT after sliding tests at 200°C. As shown in Fig. 7a, part of the worn surface becomes rough and coarse, which indicates that the materials have been removed by the sliding of Si_3N_4 ball at 200°C. As shown in Fig. 7b, the wear track morphology of NA-10WT shows a flat surface covered by a continuous tribofilm. XPS analysis of the worn surface of NA-10WT is shown in Fig. 8. It can be seen that the peaks of W and S in WS_2 are detected, indicating the existence of WS_2 in the surface layer. WS_2 is easily sheared, forming lubricious transfer films between the friction pair interface (Chhowalla and Amaratunga *(22)*). This may explain the lower coefficient of friction of NA-10WT compared to NA. However, some fine and shallow parallel grooves can also be seen on the worn surfaces. Furthermore, it is obvious that NA-10WT has a lower coefficient of friction and wear rate than NA at 200°C, which is attributed to the continuous tribofilm formed on the worn surfaces.

Figure 9 shows the wear track morphologies of NA and NA-10WT after sliding tests at 400°C. As shown in Fig. 9a, there are obvious pits and flaky wear debris adhering to the worn surface

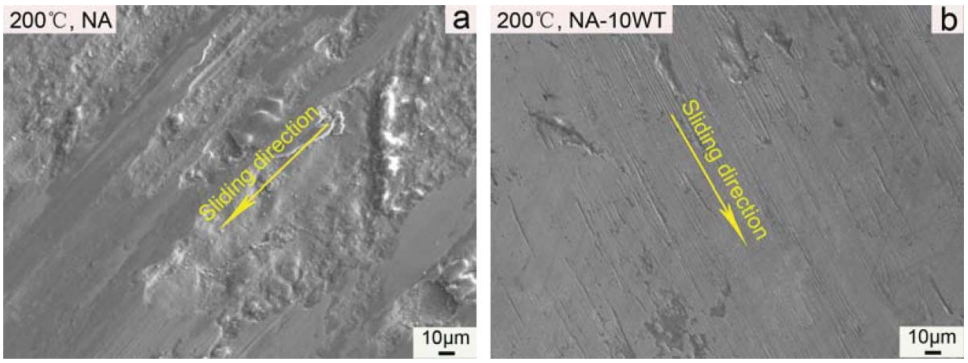

Fig. 7—Wear track morphologies of NA and NA-10WT after sliding tests at 200°C.

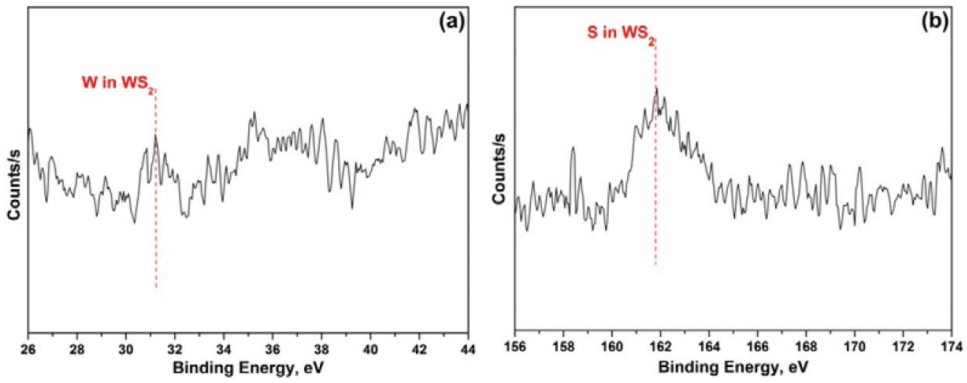

Fig. 8—XPS spectra of elements on the worn surface of NA-10WT at 200°C: (a) W and (b) S.

of NA at 400°C. The coefficient of friction of NA is observed to decrease as the temperature increases to 400°C as shown in Fig. 4a. This may be attributed to the presence of a transfer layer of wear debris, which reduces the contact between NA and the Si_3N_4 ball. At an earlier sliding friction stage, wear debris is formed between the two surfaces. Some fine equiaxed wear debris is compressed and broken into finer particles by cyclic extrusion stress. Such fine equiaxed wear debris could adhere to the worn surface of NA to form the transfer layer, which works to reduce friction. As shown in Fig. 9b, the wear track morphology of NA-10WT shows some broken grooves and a smooth film on the worn surface. The EDS analysis results show that W (5.98 wt%) and S (2.01 wt%) elements are uniformly distributed throughout the entire worn surface of NA-10WT. It can be seen that the addition of the WS_2 lubricant improves the tribological performance at temperatures from RT to 400°C. WS_2 can decrease the coefficients of friction and wear rates at relatively high temperatures because of the formation of self-lubricating films (Yang, et al. *(12)*).

Figure 10 shows the wear track morphologies of NA and NA-10WT after sliding tests at 600°C. When the temperature increases to 600°C, deep parallel distributed grooves, scattered peeling pits, and some wear particles are observed on the worn surface of NA as shown in Fig. 10a. The EDS analysis results indicate that the composition of the worn surface of NA is O13.04-A15.79-Cr3.62-Mo5.34-Ni62.21 (wt%). As shown in Fig. 10b, the worn surface is smooth and flat. It can be seen that a relatively dense tribolayer (Stott, et al. *(23)*) has been formed on the worn surface of NA-10WT. Stott, et al. *(23), (24)* and Stott *(25)* investigated the interaction between sliding wear and oxidation in superalloys. The results showed that the tribolayers could temporarily protect the surfaces from further contact damage. If they happened to wear off, new tribolayers could be formed to take their place. They reported that this progression of formation, loss, and re-formation could result in short-term friction or wear. The tribolayers have not only a significant anti-friction effect but also perform a protective action on the worn surface. Hence, NA-10WT has lower wear rate and coefficient of friction than NA at 600°C. High-temperature friction and wear is greatly reduced by the addition of Ti_3SiC_2 solid lubricant. This can be caused by a combination of adhesive transfer, viscous deformation, and oxidation wear at 600°C. The oxidation protection film of TiO_2 or mixture of TiO_2 and SiO_2 can be formed during the oxidation of Ti_3SiC_2 (Li, et al. *(26)*; Kooi, et al. *(27)*). It is well known that it is difficult to directly obtain an XRD pattern of the tribofilm on the worn surface, because X-rays can readily penetrate the tribofilm to the surface of the matrix. Hence, in order to further identify the information of element composition of the tribofilm on the worn surface, XPS analysis of the worn surface of NA-10WT was performed. From the XPS results as shown in Fig. 11, it can be seen that peaks assigned to TiO_2 and SiO_2 are detected, which indicates that the oxidation protection film of the TiO_2 and SiO_2 mixture us formed for the oxidation of Ti_3SiC_2 at high temperature. The frictional oxide film of Ti_3SiC_2

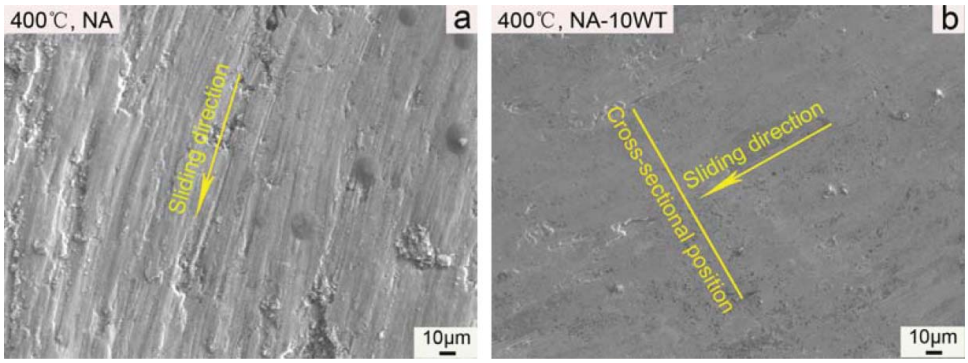

Fig. 9—Wear track morphologies of NA and NA-10WT after sliding tests at 400°C.

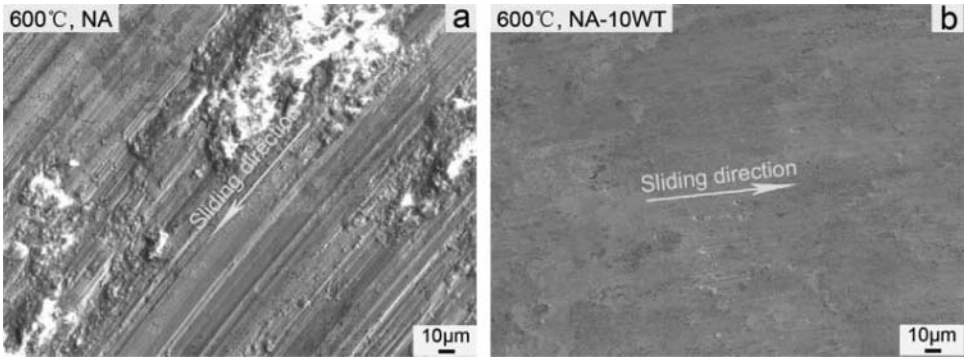

Fig. 10—Wear track morphologies of NA and NA-10WT after sliding tests at 600°C.

is adhesive as it is formed and has a significant antifriction effect. In addition, the good oxide films with a higher percentage of coverage on the friction surface result in a lower coefficient of friction and wear rate (Zhai, et al. *(28)*). Moreover, as shown in Fig. 11, the peak of W in WS_2 disappears and the peak of W in WO_3 is found, indicating that WS_2 is completely decomposed and oxidized at 600°C.

Figure 12 shows the wear track morphologies of NA and NA-10WT after sliding tests at 800°C. At 800°C, as shown in Fig. 12a, the rough worn surface of NA is mostly covered by loose debris and no grooves can be observed on the worn surface. The wear track morphology undoubtedly suggests that the dominant wear mechanism is adhesive wear. Moreover, the composition of the loose debris is O16.87-Al13.92-Cr4.14-Mo6.21-Ni58.86 (wt%) as suggested by EDS analysis. It can be speculated that the oxidation phenomenon becomes more serious with an increase in temperature, and abundant Ni-Al oxides are generated during the high-temperature reciprocating sliding process. Stott, et al. *(24)* reviewed some of the models developed to account for the generation of oxides during sliding and the effects of such oxides on the wear rates. They found that oxide was formed by the oxidation of metal asperities while in contact, and the extent of such oxidation was dependent on the temperatures developed at the asperity contacts. In addition, they claimed that oxides that occurred on the worn surface could also protect against loss of metal due to mechanical damage caused by sliding wear. However, in this study, the oxide layers on the worn surfaces of NA at elevated temperatures did not play a role in protecting the friction surface because of their loose structure and discontinuous distribution. As shown in Fig. 12b, the worn surface is

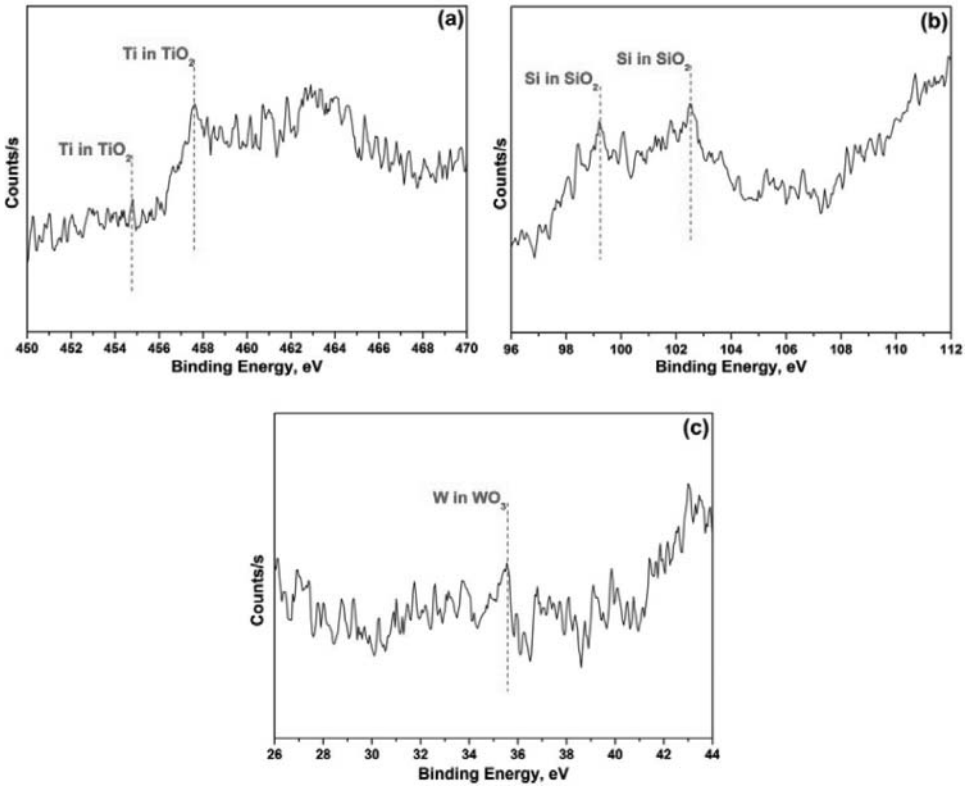

Fig. 11—XPS spectra of elements on the worn surface of NA-10WT at 600°C: (a) Ti, (b) Si, and (c) W.

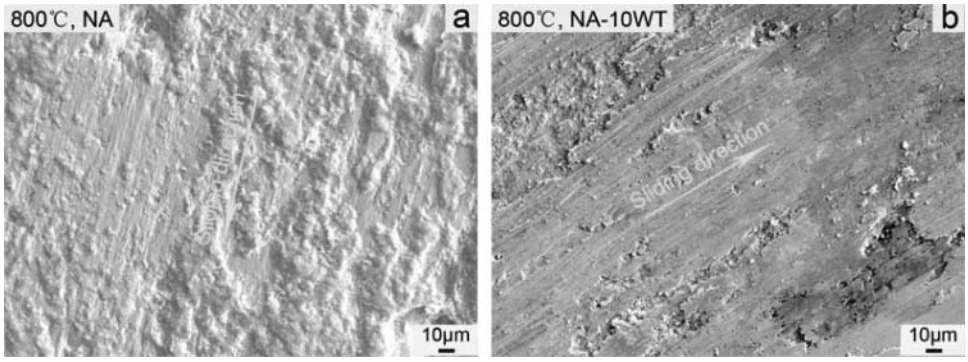

Fig. 12—Wear track morphologies of NA and NA-10WT after sliding tests at 800°C.

covered by damaged tribofilms, and some rough pits are formed for the detachment of the surface material during the sliding process. The EDS analysis reveals that the worn surface of NA-10WT consists of abundant amounts of O element (14.65 wt%). This implies that serious oxidation occurred during the sliding process. The good oxide films have an effect of solid lubrication and decrease the coefficient of friction and wear rate of NA-10WT. Zhu, et al. *(29)* reported that the formation of a continuous and dense tribofilm played a dominant role in friction reduction and antiwear properties. Tyagi, et al. *(10)* explored nickel-base composites containing nanopowders of silver and hBN. They found that the presence of a compacted transfer layer of wear debris reduced metal–metal contact and provided low-shear-strength junctions at the interface, as well as reduced the energy required to shear these junctions; hence, the coefficient of friction was reduced.

The above analysis indicates that the addition of WS_2 and Ti_3SiC_2 in the NiAl matrix as NASC is a direct and effective way to widen the operating temperature range. WS_2 plays a self-lubricating role at low and medium temperatures, and Ti_3SiC_2 is effective at high temperatures. Furthermore, the synergetic lubricating action of WS_2 and Ti_3SiC_2 is realized in NA-10WT among the as-prepared samples.

However, analysis of the worn surface morphologies of the samples is not adequate to fully explain the antiwear and friction reducing mechanisms of the additives in the NASC. It is well known that the basic factors determining the wear mechanism are chemical and structural changes that occur on and near the surface of materials (Rigney *(30)*). Plastic deformation, fracture, phase transformation, and oxidation change the microstructure and properties of surface and subsurface materials, which generate local discontinuities and microcracks and finally result in detachment of wear particles (Kolubaev, et al. *(31)*). Investigation of the microstructural evolution underneath the worn surface is quite significant in revealing the mechanism of action of the additives. In order to clarify the structure and the formation mechanism of the friction layer, subsurface analysis is carried out on the worn surface of NA-10WT obtained at 400°C by cross-sectioning it perpendicular to the sliding direction; the locations of the cross-sectional position are shown in Fig. 9c.

Figure 13 shows a typical FESEM micrograph of a cross section of the wear scar of NA-10WT after sliding at 400°C. A significant stratification morphology is easily identified, and there are three distinct layers, which are marked as A–C in Fig. 13. It can be seen that layer A is a very dense friction layer, which is beneficial to the antifriction capability and wear resistance. In the initial stage of the sliding friction process, the protrusions on the contact surfaces of NA-10WT and Si_3N_4 are difficult to either plastically deform due to their high strength and hardness or the great interfacial bond arising from the strong atomic bonds of the materials (Tang, et al. *(32)*). As the sliding friction continues, some protrusions where the shear stress is higher than the yield stress and are easily detached from NA-10WT. Under the action of continuous extrusion stress, some detached plastic particles moving between the two hard surfaces are easily smeared on the worn surface of NA-10WT, resulting in the formation of a thin friction layer on the worn surface. Layer B is composed of some submicrometer grains, whereas layer C is mainly composed of larger grains. As shown in Fig. 13, the grains show a gradual coarsening with an increasing depth from the worn surface, which is caused by the dislocation motion. This phenomenon is consistent with previous observations of the worn subsurface structure (Panin, et al. *(33)*). Figure 14 shows the microstructure and element distribution of the cross section of the wear scar of NA-10WT after sliding at 400°C obtained using EPMA. It is observed that the chemical compositions of Ni and Al are evenly distributed in different layers as shown in Figs. 14b and 14c,

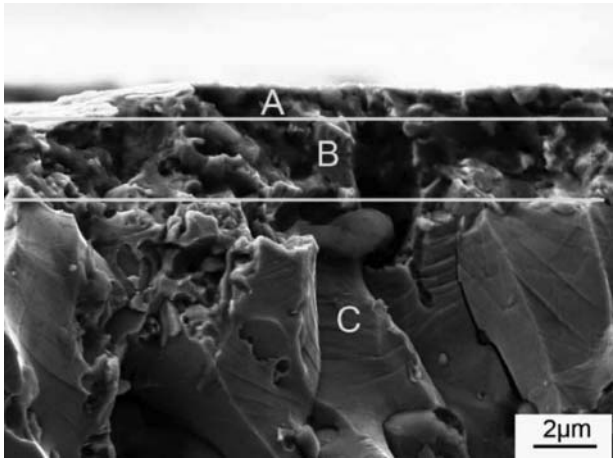

Fig. 13—Typical FESEM micrograph of the cross section of the wear scar of NA-10WT after sliding at 400°C.

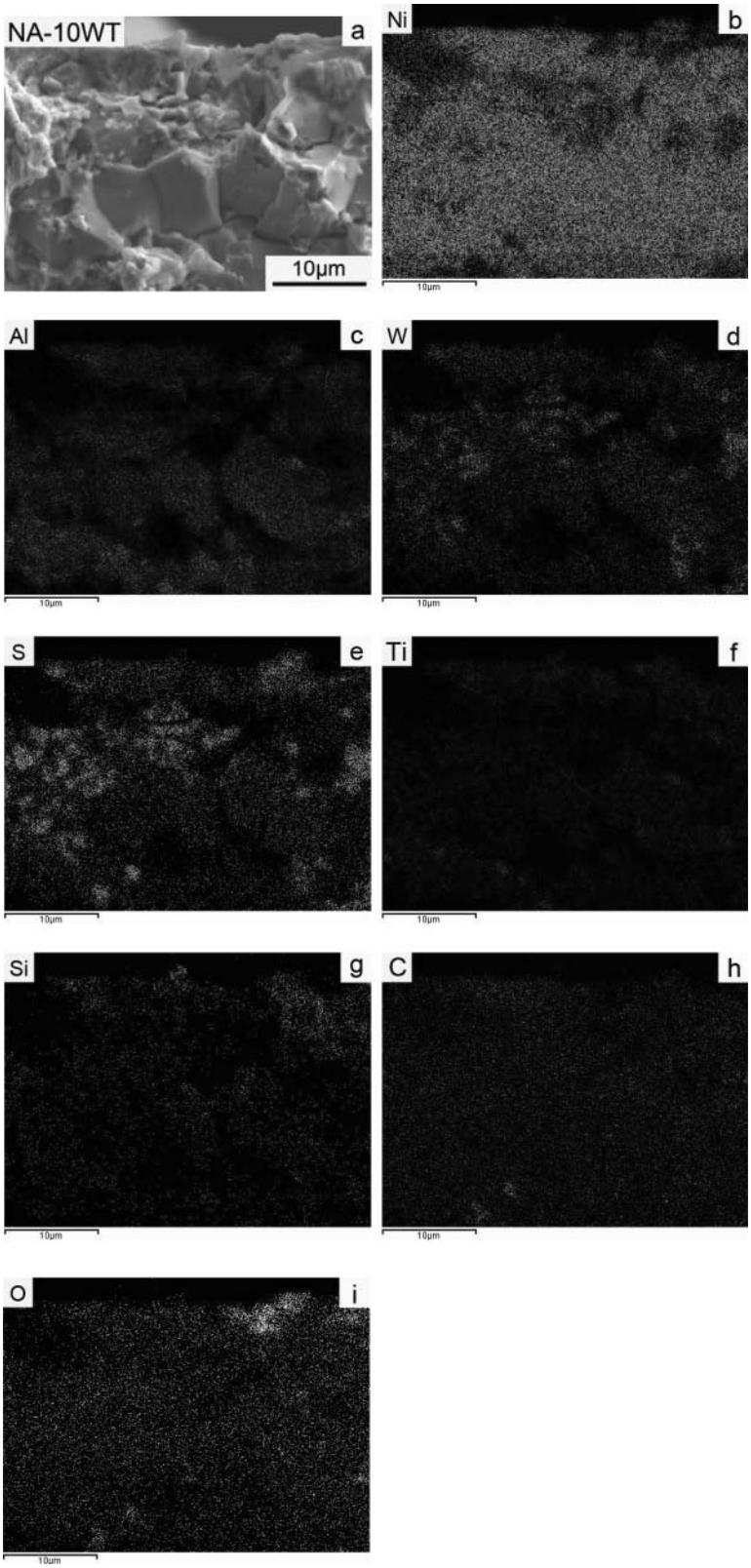

Fig. 14—Microstructure and element distribution of the cross section of the wear scar of NA-10WT after sliding at 400°C.

corresponding to the NiAl substrate. As shown in Figs. 14d–14i, Ti, Si, C, W, S, and O are enriched in regions A and B. It could be concluded that Ti_3SiC_2 and WS_2, which are added as the lubricants, are beneficial to the formation of an antifriction film on the worn surface. It is obvious that NA-10WT have lower coefficients of friction and wear rates than NA at 400°C, indicating that the solid lubricants of WS_2 and Ti_3SiC_2 played an excellent role in lubrication during the sliding process of the Si_3N_4 ball on

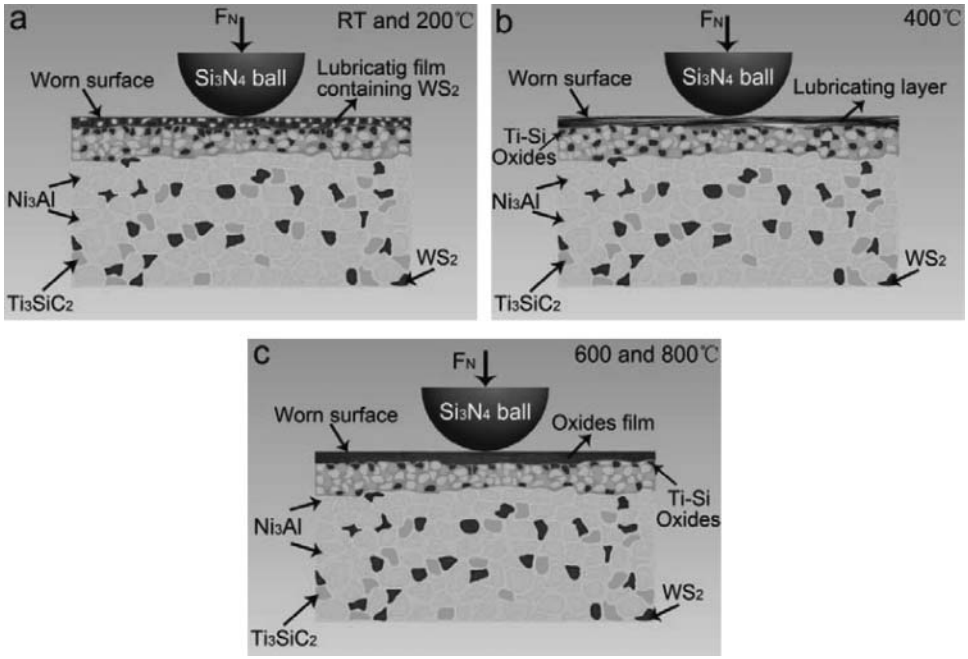

Fig. 15—Schematic illustration of the wear mechanisms of NA-10WT during the sliding process at different temperatures.

the same worn surface of NA-10WT. WS_2 is characterized by weak interatomic interactions between the layered structures and is easily sheared, forming a lubricious transfer film between the friction pair interface (Chhowalla and Amaratunga *(22)*). Therefore, WS_2 easily overcomes the potential barrier of NiAl substrate and accumulates near the frictional contact surface under the action of continuous extrusion stress and cyclic shear stress. Moreover, the presence of O element indicates that a mild oxidation reactions occur. The oxidation protection film of TiO_2 or mixture of TiO_2 and SiO_2, which are beneficial in reducing the coefficient of friction and wear rate, can form for the oxidation of Ti_3SiC_2 (Li, et al. *(34)*). As shown in Fig. 13, a dense friction layer is formed on the worn surface of NA-10WT. The friction layer containing abundant WS_2 and Ti-Si oxides reduces direct contact between the Si_3N_4 ball and NA-10WT and provides low-shear-strength junctions at the interface, as well as decreases the friction between the Si_3N_4 ball and NA-10WT; hence, the coefficient of friction and wear rate are reduced. According to the aforementioned analysis, WS_2 and Ti_3SiC_2, which are added as lubricants, are beneficial to the formation of an antifriction layer on the worn surface. The coefficient of friction and wear rate of NA-10WT are decreased with the formation of this antifriction layer, indicating that WS_2 and Ti_3SiC_2 play an excellent role in lubrication in NA-10WT.

Figure 15 is a schematic illustration that shows the wear mechanisms of NA-10WT during the sliding process at different temperatures. WS_2, a low-temperature solid lubricant, plays a dominant role in lubrication at RT and 200°C. As shown in Fig. 15a, lamellar WS_2 particles overcome the potential barriers and accumulate near the sliding surface during the friction process. Under the action of continuous extrusion stress, some detached plastic particles including WS_2 particles are easily smeared on the worn surface of NA-10WT, resulting in the formation of a lubricating film. The friction layer forms low-shear-stress junctions at the sliding interface, which not only has a significant antifriction effect but also has a protective action on the worn surface. As the temperature increases to 400°C, as shown in Fig. 15b, the mild oxidation phenomenon proceeds during the continuous sliding process. Ti-Si oxides are formed for the oxidation of Ti_3SiC_2. At 400°C, a dense friction layer containing abundant WS_2 and Ti-Si oxides is formed on the worn surface. It effectively isolates the friction between the sample and Si_3N_4 ball, which is beneficial to the lower coefficient of friction and wear rate. As the temperatures approach or exceed 600°C, the oxidation phenomenon becomes more serious during the sliding process. Under the action of cyclic shear stress and continuous extrusion stress, the oxides would be scaled off and then smeared on the worn surface. The oxide layer mainly containing Ti-Si oxides has a significant antifriction effect on the friction surface and protects the worn surface. The coefficient of friction and wear rate of NA-10WT are decreased with the formation of this antifriction layer. According to the above analysis, we can conclude that the WS_2 lubricant is squeezed out from the matrix and forms a lubricating film on the worn surfaces below 400°C, which contributes to the lower coefficient of friction and wear rate of NA-10WT at low temperature. With an increase in temperature, the oxidation phenomenon becomes more serious, and WS_2 lubricant is completely decomposed and oxidized. In addition, a new friction layer is formed at higher temperatures, mainly containing Ti-Si oxides, and replaces the lubricating film containing WS_2 to continuously protect the worn surface. The self-lubrication properties of NA-10WT in a wide temperature range are realized by WS_2 at low temperatures ranging from RT to 400°C, as well as Ti_3SiC_2 at high temperatures ranging from 400 to 800°C. Hence, adding WS_2 and Ti_3SiC_2 into the Ni_3Al matrix

self-lubricating composites is a direct and effective way to widen the operating temperature range.

CONCLUSIONS

The dry friction and wear behaviors of NASC containing varying amounts of WT sliding against an Si_3N_4 ball at temperatures from RT to 800°C were systematically researched. The wear and lubrication mechanisms were investigated according to the analysis of the morphologies and compositions of the worn surfaces and cross section of the wear scar. The main conclusions were as follows:

1. The tribological properties of NASC were improved by adding composite solid lubricants WS_2 and Ti_3SiC_2. The coefficients of friction and wear rates of NASC containing WS_2 and Ti_3SiC_2 were lower than those of Ni_3Al alloy over a wide temperature range.
2. WS_2 can provide good lubricity at temperatures from RT to 400°C and Ti_3SiC_2 can provide good lubricity at temperatures above 400°C. The synergetic lubricating effect of WS_2 and Ti_3SiC_2 ensured that NASC possessed a low coefficient of friction and wear rate over a wide temperature range.
3. NA-10WT exhibited the best self-lubricating performance and tribological properties in comparison with other composites. When the test temperature increased from RT to 800°C, the coefficients of friction were in the range of 0.18–0.31 and the wear rates were in the range of 1.5–3.1 ċ 10^{-5} $mm^3N^{-1}m^{-1}$.
4. NASC containing WS_2 and Ti_3SiC_2 showed excellent tribological properties from RT to 800°C, which was attributed to the formation of the lubricating layer on the worn surface during the sliding process. The lubricating film formed low-shear-stress junctions at the sliding interface, which not only had a significant antifriction effect but also had a protective action on the worn surface below 400°C. When the temperature was above 400°C, a friction layer containing Ti-Si oxides had a significant antifriction effect on the friction surfaces and continuously protected the worn surfaces.

FUNDING

This work was supported by the Nature Science Foundation of Hubei Province (2012FFB05104); the National Natural Science Foundation of China (51275370); the Fundamental Research Funds for the Central Universities (2014-yb-004); the Project for Science and Technology Plan of Wuhan City (2013010501010139); the Academic Leader Program of Wuhan City (201150530146); and the Project for Teaching and Research project of Wuhan University of Technology (2012016).

REFERENCES

(1) Berman, D., Erdemir, A., and Sumant, A. V. (2014), "Graphene: A New Emerging Lubricant," *Materials Today*, **17** (1), pp 31–42.
(2) Evans, D. C. and Senior, G. S. (1982), "Self-Lubricating Materials for Plain Bearing," *Tribology International*, **15** (5), pp 243–248.
(3) Prasad, S. V. and Mecklenburg, K. R. (1996), "Characterization of Third Bodies in Self-Lubricating Aluminum Metal-Matrix Composites by Electron Microprobe Analysis," *Tribology Transactions*, **39** (2), pp 296–305.
(4) Sierra, C. and Vazquez, A. J. (2006), "Dry Sliding Wear Behavior of Nickel Aluminides Coatings Produced by Self-Propagating High-Temperature Synthesis," *Intermetallics*, **14** (7), pp 848–852.
(5) Zhu, S. Y., Bi, Q. L., Kong, L. Q., Yang, J., and Liu, W. M. (2012), "Barium Chromates as a Solid Lubricants for Nickel Aluminum," *Tribology Transactions*, **55** (2), pp 218–223.
(6) Li, J. L., Xiong, D. S., Huang, Z. J., Kong, J., and Dai, J. H. (2009), "Effect of Ag and CeO_2 on Friction and Wear Properties of Ni-Base Composite at High Temperature," *Wear*, **267** (1), pp 576–584.
(7) Sliney, H. E. (1982), "Solid Lubricant Materials for High Temperatures—A Review," *Tribology International*, **15** (5), pp 303–315.
(8) Ouyang, J. H., Li, Y. F., Wang, Y. M., Zhou, Y., Murakami, T., and Sasaki, S. (2009), "Microstructure and Tribological Properties of ZrO_2 (Y_2O_3) Matrix Composites Doped with Different Solid Lubricants from Room Temperature to 800°C," *Wear*, **267** (9), pp 1353–1360.
(9) Dellacorte, C. (2000), "The Evaluation of a Modified Chrome Oxide Based High Temperature Solid Lubricant Coating for Foil Gas Bearings," *Tribology Transactions*, **43** (2), pp 257–262.
(10) Tyagi, R., Xiong, D. S., Li, J. L., and Dai, J. H. (2010), "Elevated Temperature Tribological Behavior of Ni Based Composites Containing Nano-Silver and hBN," *Wear*, **269** (11), pp 884–890.
(11) Zhu, S. Y., Bi, Q. L., Yang, J., Liu, W. M., and Xue, Q. J. (2011), "Ni_3Al Matrix High Temperature Self-Lubricating Composites," *Tribology International*, **44** (4), pp 445–453.
(12) Yang, M. S., Liu, X. B., Fan, J. W., He, X. M., Shi, S. H., Fu, G. Y., Wang, M. D., and Chen, S. F. (2012), "Microstructure and Wear Behaviors of Laser Clad NiCr/Cr_3C_2-WS_2 High Temperature Self-Lubricating Wear-Resistant Composite Coating," *Applied Surface Science*, **258** (8), pp 3757–3762.
(13) Shi, X. L., Wang, M., Xu, Z. S., Zhai, W. Z., and Zhang, Q. X. (2013), "Tribological Behavior of Ti_3SiC_2/(WC-10Co) Composites Prepared by Spark Plasma Sintering," *Materials & Design*, **45**, pp 365–376.
(14) Zhang, Y., Ding, G. P., Zhou, Y. C., and Cai, B. C. (2002), "Ti_3SiC_2—A Self-Lubricating Ceramic," *Materials Letters*, **55** (5), pp 285–289.
(15) Shi, X. L., Zhai, W. Z., Wang, M., Xu, Z. S., Yao, J., Song, S. Y. and Zhang, Q. X. (2014), "Tribological Behaviors of NiAl-Ti_3SiC_2 Self-Lubricating Composites at Elevated Temperatures," *Tribology Transactions*, **57** (4), pp 589–602.
(16) Barsoum, M. W., El-Raghy, T., and Ogbuji, L. U. (1997), "Oxidation of Ti_3SiC_2 in Air," *Journal of the Electrochemical Society*, **144** (7), pp 2508–2516.
(17) Peng, M. C., Shi, X. L., Zhu, Z. W., Wang, M., and Zhang, Q. X. (2012), "Facile Synthesis of Ti_3SiC_2 Powder by High Energy Ball-Milling and Vacuum Pressureless Heat-Treating Process from Ti-TiC-SiC-Al Powder Mixtures," *Ceramics International*, **38** (3), pp 2027–2033.
(18) American Society for Testing and Materials. (2013), "Standard Test Methods for Density of Compacted or Sintered Powder Metallurgy (PM) Products Using Archimedes' Principle," **ASTM B962–13**.
(19) American Society for Testing and Materials. (2013), "Standard Test Methods for Knoop and Vickers Hardness of Materials," **ASTM E384–11e1**.
(20) American Society for Testing and Materials. (2005), "Standard Test Method for Wear Testing with a Pin-on-Disk Apparatus," **ASTM G99–05**.
(21) Yang, J., Gu, W., Pan, L. M., Song, K., Chen, X., and Qiu, T. (2011), "Friction and Wear Properties of in situ (TiB_2 + TiC)/Ti_3SiC_2 Composites," *Wear*, **271** (11), pp 2940–2946.
(22) Chhowalla, M. and Amaratunga, G. A. J. (2000), "Thin Films of Fullerene-Like MoS_2 Nanoparticles with Ultra-Low Friction and Wear," *Nature*, **407** (6801), pp 164–167.
(23) Stott, F. H., Lin, D. S., and Wood, G. C. (1973), "Glazes" Produced on Nickel-Base Alloys during High Temperature Wear," *Nature*, **242** (118), pp 75–77.
(24) Stott, F. H., Lin, D. C., and Wood, G. C. (1973), "Structure and Mechanism of Formation of the 'Glaze' Oxide Layers Produced on Ni-Based Alloys during Wear at High Temperatures," *Corrosion Science*, **13** (6), pp 449–469.
(25) Stott, F. H. (1998), "The Role of Oxidation in the Wear of Alloys," *Tribology International*, **31** (1), pp 61–71.
(26) Li, S. B., Xie, J. X., Zhang, L. T., and Cheng, L. F. (2003), "Mechanical Properties and Oxidation Resistance of Ti_3SiC_2/SiC Composite Synthesized by in situ Displacement Reaction of Si and TiC," *Materials Letters*, **57** (20), pp 3048–3056.

(27) Kooi, B. J., Poppen, R. J., Carvalho, N. J. M., De Hosson, J. T. M., and Barsoum M. W. (2003), "Ti_3SiC_2: A Damage Tolerant Ceramic Studied with Nano-Indentations and Transmission Electron Microscopy," *Acta Materialia*, **51** (10), pp 2859–2872.

(28) Zhai, H. X., Huang, Z. Y., and Ai, M. X. (2006), "Tribological Behaviors of Bulk Ti_3SiC_2," *Materials Science and Engineering A*, **435>–436**, pp 360–370.

(29) Zhu, S. Y., et al. (2012), "Tribological Behavior of NiAl Matrix Composites with Addition of Oxides at High Temperatures," *Wear*, **274–275**, pp 423–434.Please provide all author names, reference 29

(30) Rigney, D. A. (1997), "Comments on the Sliding Wear of Metals," *Tribology International*, **30** (5), pp 361–367.

(31) Kolubaev, A., Tarasov, S., Sizova, O., and Kolubaev E. (2010), "Scale-Dependent Subsurface Deformation of Metallic Materials in Sliding," *Tribology International*, **43** (4), pp 695–699.

(32) Tang, H. B., Fang, Y. L., and Wang, H. M. (2004), "Microstructure and Dry Sliding Wear Resistance of a $Cr_{13}Ni_5Si_2$ Ternary Metal Silicide Alloy," *Acta Materialia*, **52** (7), pp 1773–1783.

(33) Panin, V., Kolubaev, A., Tarasov, S., and Popov, V. (2001), "Subsurface Layer Formation during Sliding Friction," *Wear*, **249** (10), pp 860–867.

(34) Li, S. B., Cheng, L. F., and Zhang, L. T. (2003), "The Morphology of Oxides and Oxidation Behavior of Ti_3SiC_2-Based Composite at High-Temperature," *Composites Science and Technology*, **63** (6), pp 813–819.